Journal of the University of Chemical Technology and Metallurgy, 44, 3, 2009, 307-312

ESTIMATION OF MIXING RATIOS OF THREE COMPONENT MIXTURE USING SHEAR HORIZONTAL SURFACE ACOUSTIC WAVE SENSOR AND NEURAL NETWORK

T. E. Taha[1], M. A. A. El-Dosoky [2], A. M. El-Sayed[2]

[1] *Communication Department, Faculty of Electronic Engineering, Menoufia University, Menouf, Egypt.*

[2] *Biomedical Department, Faculty of Engineering, Helwan University, Helwan, Egypt.*
E-mail: bio_eng_ahmed@hotmail.com

Received 25 May 2009
Accepted 23 July 2009

ABSTRACT

Recently, Surface Acoustic Waves (SAW) are developed and used in many applications. The estimation of the mixed electrolytes is one of these applications. This is done by using a flow of this solution passed between two interdigital transducers of SAW sensor. A certain kind of SAW will be generated called Shear Horizontal (SH-SAW). This wave is very sensitive to these solutions, where clear perturbations in the attenuation and the frequency shifts of the received signal are observed. Experimental results of the liquid flow system with SH-SAW sensor are taken. From this data, an algorithm is proposed with the aid of feed-forward backpropagation neural network that will be used directly to identify the three components of ions and determine the mixing ratio between the electrolytes. The durations of time responses, Fast Fourier Transform (FFT), and Discrete Cosine Transform (DCT) are used as features in this algorithm.

Keywords: Surface Acoustic Wave (SAW), Neural Network, Fast Fourier Transform (FFT), Discrete Cosine Transform (DCT).

INTRODUCTION

Currently, surface acoustic waves (SAW) devices are widely used in many applications, such as in determining the properties of gases [1,2], liquids [3-5] and thin films [6]. Recently, SAW stated its role in medicine, where SAW devices are used to early cancer detection [7]. Also SAW devices can be used as biomedical sensors to detect biological materials as: DNA [8,9], bacteria [10, 11], viruses [12,13], proteins [13, 14], and enzymes [15, 16].

A surface acoustic wave (SAW) is an acoustic wave traveling along the surface of a material having some elasticity, with an amplitude that typically decays exponentially with the depth of the substrate.

The most common mode of SAW is Shear Horizontal Surface Acoustic Wave (SH-SAW). In this mode, the propagation of the wave is on the top of the substrate and normal to wave displacement, as shown in Fig.1 [17]. Disappearing the normal component of SAW allows shear horizontal mode to propagate and contact with a liquid on the surface. Consequently, the interaction between the surface wave and the liquid causes the most sensitive variation in the characteristics of the received SAW.

The SAW is generated by using an exciting transducer called Inter-digital transducer (IDT). The general configuration of it is shown in Fig.1 with two groups of fingers, one for generating and transmitting SAW and the other for receiving the perturbed waves. These trans-

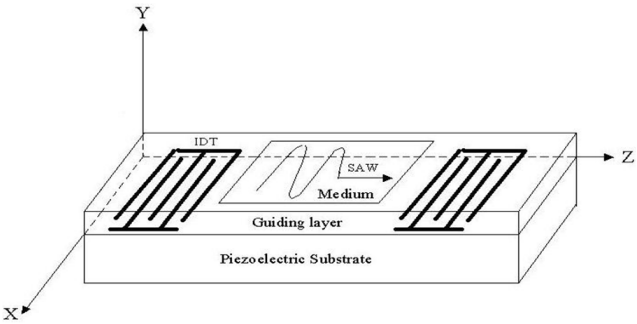

Fig. 1. Scheme of SAW device showing the shear horizontal (SH) displacement of the mode as it propagates between input and output inter-digital transducers.

ducers are on a piezoelectric substrate. The finger width, d, of the IDT determines the acoustic wavelength, λ, where [18, 19]:

$$\lambda = 4d \tag{1}$$

The fundamental resonance frequency of the SAW device is determined as:

$$f_0 = \frac{v_0}{\lambda} \tag{2}$$

where f_0 and v_0 are the unperturbed frequency and the unperturbed velocity respectively.

Besides the simplicity in the structure of the SAW devices, they have the following advantages [19]:

1. SAW devices can be designed to provide complicated signal processing functions with a fairly simple structure (a single piezoelectric substrate with normally two IDTs).

2. A broad range of response functions can be obtained through variation of electrode patterns.

3. Outstanding reproducibility and accuracy.

4. Most SAW devices are manufactured using single-stage lithography, which is ideal for mass production of low-cost devices.

5. SAW devices can be miniaturized in micro and nano scale with stable characteristics.

As the SAW propagates along the surface of piezoelectric substrate, it will interact with the medium. This medium may be thin film or liquid or gas. Depending on the physical properties of the medium, certain changes in the velocity and the amplitude of the wave will relate to them.

This interaction causes changes in the velocity and/or the attenuation of the SAW. According to the perturbation theory, the following relationships are derived by using one of the used SAW models (equivalent circuit model or electromagnetic model) [18]:

$$\frac{\Delta v}{v_0} \approx -\frac{K^2}{2}\frac{1}{1+[v_0 C_s/\sigma_m]^2} \tag{3}$$

$$\frac{\Delta \alpha}{\kappa} \approx \frac{K^2}{2}\frac{v_0 C_s/\sigma_m}{1+[v_0 C_s/\sigma_m]^2} \tag{4}$$

Where $\Delta v/v0$ is the perturbation in the velocity, $\Delta\alpha/\kappa$ is the attenuation, K^2 is the electromechanical coupling coefficient, $v0$ is the unperturbed velocity of SAW, σm is the medium conductivity and C_s is the surface capacitance per unit length (the sum of dielectric constants of the piezoelectric substrate and the medium).

The Fast Fourier Transform (FFT) is a family of very efficient algorithms for computing the Discrete Fourier Transform (DFT). FFT is simply an efficient algorithm extracting from the DFT by taking advantage of the fact that many computations are repeated in the DFT because of the periodic nature of the twiddle factors. The ratio of computing cost in terms of number of multiplications is approximately as the following [20]:

$$\frac{DFT}{FFT} = \frac{\log_2 N}{2N} \tag{5}$$

Then the Discrete Fourier Transform equation is given as following [21]:

$$x(\omega) = \sum_{n=-\infty}^{\infty} x(n) e^{-j\omega n} \tag{6}$$

where $x(n)$ is the sampled signal, ω ranges from 0 to 2π and $x(\omega)$ is periodic with 2π.

The Discrete Cosine Transform (DCT) is a technique for converting the signal into elementary frequency components [22]. The DCT is a transform similar to the DFT, except that it uses only the real part of the signal. This is possible because the Fourier series of a real and even signal function has only cosine terms. The DCT can be obtained by taking the transform of the real part giving for $k = 1, 2, \ldots, N$:

$$x_c(k) = Re\left[\sum_{n=1}^{N} x_n e^{-\frac{j2\pi nk}{N}}\right] = \sum_{n=1}^{N} x_n \cos\left(\frac{2\pi kn}{N}\right) \quad (7)$$

In [23], the investigators can determine the components of the solution using the curves by checking the point of interaction between the curves of the attenuation and the velocity shifts. From this point, they can determine the presence of each electrolyte in the solution or not.

In this paper, we concentrate on the features that give the main differences and enable us to differentiate among three different kinds of electrolytes and determine the ratio of each electrolyte to the other in each mixture from only one curve, the attenuation or the frequency shift curve not the two curves as in [23]. This is done by building a computer programs using the feed-forward backpropagation neural network to identify and estimate the components of ions, and mixing ratio of KCl, NaCl and $BaCl_2$ of mixture solutions which have the same conductivity. The core data is taken from experimental results using a liquid flow system with SH-SAW sensor [23,24].

METHOD AND FEATURES EXTRACTION

An Artificial Neural Network (ANN) is used for identification [25]. In this network, the information moves in only one direction, forward, from the input neurons, through the hidden neurons and to the output neurons. There are no cycles or loops in the network.

Here, all solutions and the mixtures have the same conductivity that is equal to 0.5 S/m. the attenuation response for these solutions is shown in Fig.2. The solid line is for the KCl solution and the next dot one is for NaCl. The area between them is related to the ratio between these solutions. This is also repeated for the next dot curve that is for $BaCl_2$ solution. This data is taken from experimental results using a liquid flow system with SH-SAW sensor [23, 24].

There are three types of feature extraction from attenuation ($\Delta\alpha/\kappa$) curves. Firstly, the relative duration of attenuation ($\Delta\alpha/\kappa$) curves of mixing ratios of KCl, NaCl and $BaCl_2$ solution. From Fig.2, it is shown that this width changes as changing the ratio of the solutions. Secondly and thirdly, since these curves are in time domain, the fast Fourier Transform (FFT) and the Discrete Cosine Transform (DCT) can be used as signal processing tools for analyzing these responses.

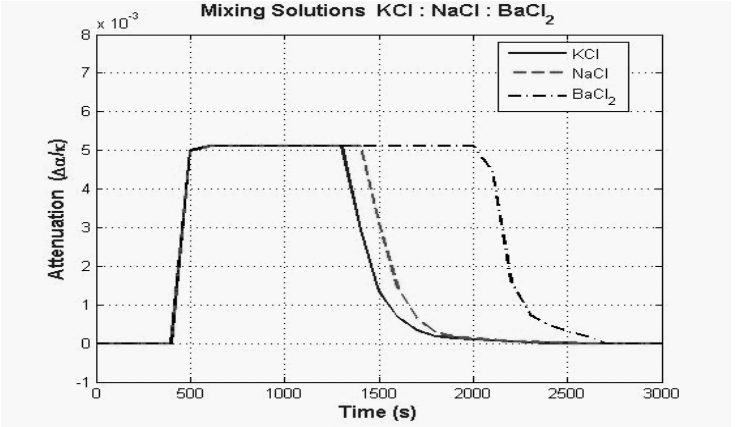

Fig. 2. The attenuation responses for the solutions with the same conductivity.

The preparing of attenuation ($\Delta\alpha/\kappa$) curves of mixing ratios of KCl, NaCl and $BaCl_2$ solution which has the same conductivity ($\sigma = 0.5$ S/m) is discussed as following steps:

1. Take the attenuation ($\Delta\alpha/\kappa$) curves from experimental results (3 attenuation ($\Delta\alpha/\kappa$) curves of mixing ratios of KCl, NaCl and $BaCl_2$ are 100:0:0, 0:100:0 and 0:0:100) as shown in Fig.2 [23].

2. Draw linear curves between mixing ratios of KCl, NaCl and $BaCl_2$ mixture solution of attenuation ($\Delta\alpha/\kappa$) curves vs. duration at 0.0051, 0.005, 0.004, 0.003, 0.002, 0.001 and 0.0005 ppm's for curves between 100:0:0 and 0:100:0 mixing ratios of KCl, NaCl and $BaCl_2$ mixture solutions of attenuation ($\Delta\alpha/\kappa$) curves, and also for curves between 0:100:0 and 0:0:100 mixing ratios. As shown in Fig.3, there are two sample curves (a) 0.0051 ppm for curves between 100:0:0 and 0:100:0 mixing ratios of KCl, NaCl and $BaCl_2$ solutions of attenuation ($\Delta\alpha/\kappa$) curves, and (b) 0.0051 ppm for curves between 0:100:0 and 0:0:100 mixing ratios of KCl, NaCl and $BaCl_2$ solutions of attenuation ($\Delta\alpha/\kappa$) curves.

3. According to previous step, 21 curves of attenuation ($\Delta\alpha/\kappa$) curves (mixing ratios of KCl, NaCl and $BaCl_2$ are 100:0:0, 90:10:0, 80:20:0, 70:30:0, 60:40:0, 50:50:0, 40:60:0, 30:70:0, 20:80:0, 10:90:0, 0:100:0, 0:90:10, 0:80:20, 0:70:30, 0:60:40, 0:50:50, 0:40:60, 0:30:70, 0:20:80, 0:10:90 and 0:0:100) are drawn by program. This step to increase the numbers of curves

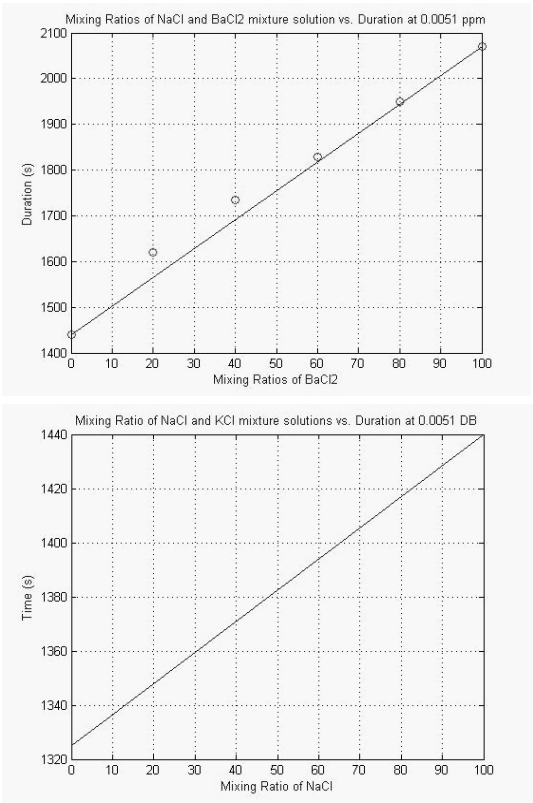

Fig. 3. Linear curves between mixing ratios of KCl, NaCl and $BaCl_2$ solution of attenuation ($\Delta a/k$) curves vs. duration at (a) 0.0051 ppm for curves between 100:0:0 and 0:100:0 mixing ratios of KCl, NaCl and $BaCl_2$ mixture solutions of attenuation ($\Delta a/k$) curves. (b) 0.0051 ppm for curves between 0:100:0 and 0:0:100 mixing ratios of KCl, NaCl and $BaCl_2$ mixture solution s of attenuation ($\Delta a/k$) curves.

to use it as training and testing curves in neural network stage.

According to the preparing of attenuation ($\Delta\alpha/\kappa$) curves of mixing ratios of KCl, NaCl and $BaCl_2$ mixture solution, the features extraction for each curve is discussed as following steps:

1. Determine the relative duration for each attenuation ($\Delta\alpha/\kappa$) curve at 0.0051, 0.005, 0.004, 0.003, 0.002, 0.001 and 0.0005 ppm's of attenuation ($\Delta\alpha/\kappa$) curves to 0.0051 ppm of attenuation ($\Delta\alpha/\kappa$) curve of mixing ratio of KCl, NaCl and $BaCl_2$ 0:100:0 mixture solution.

2. Get real Fast Fourier Transform (FFT), then get maximum, minimum, median, standard deviation and covariance values relative to the maximum value of FFT of attenuation ($\Delta\alpha/\kappa$) curve of mixing ratio of KCl, NaCl and $BaCl_2$ 0:100:0 mixture solution.

3. Get absolute Fast Fourier Transform (FFT), then get minimum, mean, median, standard deviation and covariance values relative to the maximum value of FFT of attenuation ($\Delta\alpha/\kappa$) curve of mixing ratio of KCl, NaCl and $BaCl_2$ 0:100:0 mixture solution.

4. Get real Discrete Cosine Transform (DCT), then get maximum, minimum, mean, median, standard deviation and covariance values relative to the maximum value of FFT of attenuation ($\Delta\alpha/\kappa$) curve of mixing ratio of KCl, NaCl and $BaCl_2$ 0:100:0 mixture solution.

5. Get absolute Discrete Cosine Transform (DCT), then get minimum, mean, median, standard deviation and covariance values relative to the maximum value of FFT of attenuation ($\Delta\alpha/\kappa$) curve of mixing ratio of KCl, NaCl and $BaCl_2$ 0:100:0 mixture solution.

TRAINING AND RESULTS

In the training step, the feed-forward backpropagation neural network is used in this program. The input layer of neural network has 35 neurons, the hidden layer has selected 4, 5, 6, 7, 8 and 9 neurons and the output layer has 3 neurons. The first, the second and the third neuron of output layer for mixing ratio of KCl, NaCl and $BaCl_2$, respectively. The schematic configuration of the feed-forward backpropagation neural network which use in this paper is shown in Fig. 4.

The training is done for the 15 attenuation ($\Delta\alpha/\kappa$) curves of mixing ratios of KCl, NaCl and $BaCl_2$ mixture solution, mixing ratios of KCl, NaCl and $BaCl_2$ are 100:0:0, 90:10:0, 70:30:0, 60:40:0, 40:60:0, 30:70:0, 10:90:0, 0:100:0, 0:90:10, 0:70:30, 0:60:40, 0:40:60, 0:30:70, 0:10:90 and 0:0:100, each curve has a matrix contain all features which described previously.

In the test step, the 15 attenuation ($\Delta\alpha/\kappa$) curves of mixing ratios of KCl, NaCl and $BaCl_2$ (mixing ratios

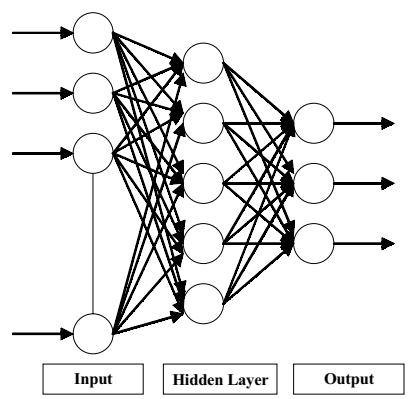

Fig. 4. The scheme configuration of the feed-forward backpropagation neural network which use in this paper.

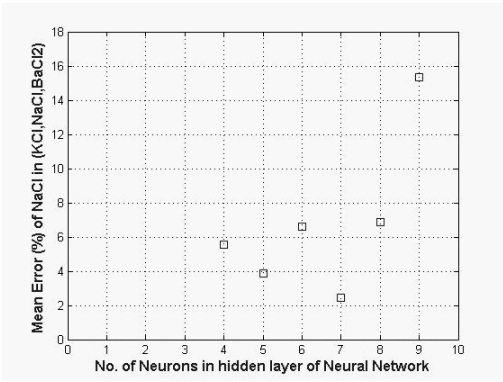

Fig. 5. The results of mean error of NaCl in KCl, NaCl and $BaCl_2$ solution for all numbers of neurons (4, 5, 6, 7, 8 and 9) in hidden layer of the feed-forward backpropagation neural network.

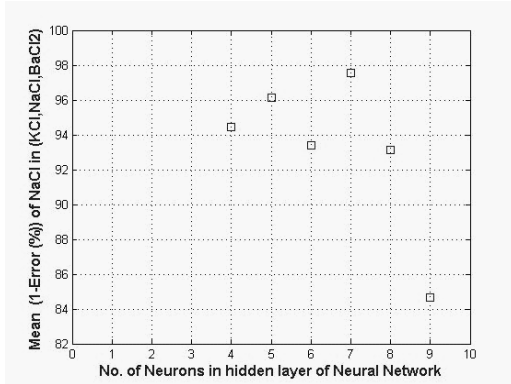

Fig. 6. The results of mean correction (1 – error) of NaCl in KCl, NaCl and $BaCl_2$ solution for all numbers of neurons (4, 5, 6, 7, 8 and 9) in hidden layer of the feed-forward backpropagation neural network.

Table.1. The all results (mixing ratios for KCl, NaCl and $BaCl_2$, errors and corrections) for all numbers of neurons (4, 5, 6, 7, 8 and 9) in hidden layer of the feed-forward backpropagation neural network.

No. of hidden layer		4	5	6	7	8	9
(80,20,0)	KCl	80.470	80.521	81.317	80.501	78.563	83.819
	NaCl	20.230	21.095	18.766	19.507	22.688	16.150
	$BaCl_2$	-0.700	-1.616	-0.083	-0.008	-1.252	0.030
(50,50,0)	KCl	46.886	47.648	47.195	48.604	50.111	49.628
	NaCl	52.084	49.605	52.685	51.277	47.819	50.375
	$BaCl_2$	1.029	2.745	0.118	0.118	2.068	-0.004
(20,80,0)	KCl	20.851	20.420	20.409	20.170	21.271	21.896
	NaCl	79.257	79.268	79.562	79.851	78.706	78.104
	$BaCl_2$	-0.108	0.310	0.028	-0.021	0.022	-0.0006
(0,80,20)	KCl	4.681	1.524	-2.419	6.415	-2.726	$-4X10^{6}$
	NaCl	76.266	83.315	85.640	77.490	86.243	91.205
	$BaCl_2$	19.051	15.160	16.779	16.093	16.482	8.794
(0,50,50)	KCl	-6.857	-8.097	-3.549	-3.358	-6.314	-10^{-5}
	NaCl	52.985	53.078	49.420	52.258	49.938	38.982
	$BaCl_2$	53.872	55.019	54.128	51.099	56.376	61.017
(0,20,80)	KCl	8.373	9.637	3.373	3.099	3.300	10^{-5}
	NaCl	16.684	18.823	23.894	20.389	22.800	26.710
	$BaCl_2$	74.941	71.539	72.732	76.510	73.898	73.289
Mean NaCl Error (%)		5.576	3.893	6.627	2.4676	6.892	15.327
Mean NaCl 1-Error (%)		94.423	96.106	93.372	97.5323	93.107	84.672

of KCl, NaCl and $BaCl_2$ are 100:0:0, 90:10:0, 70:30:0, 60:40:0, 40:60:0, 30:70:0, 10:90:0, 0:100:0, 0:90:10, 0:70:30, 0:60:40, 0:40:60, 0:30:70, 0:10:90 and 0:0:100) mixture solution is tested for all numbers of neurons (4, 5, 6, 7, 8 and 9) in hidden layer of feed-forward backpropagation neural network. For each test for each attenuation ($\Delta\alpha/\kappa$) curve, the error is 0 % and the correction (1-error) is 100 %.

In this program, the selected attenuation ($\Delta\alpha/\kappa$) curves which has mixing ratio of KCl, NaCl and $BaCl_2$ 80:20:0, 50:50:0, 20:80:0, 0:80:20, 0:50:50 and 0:20:80 mixture solution are used in the test step. The mean error results of NaCl in KCl, NaCl and $BaCl_2$ mixture solutions are shown in Fig. 5, the mean correction (1 – error) results of NaCl in KCl, NaCl and $BaCl_2$ mixture solution is shown in Fig.6, and all results (mixing ratios of KCl, NaCl and $BaCl_2$ are 80:20:0, 50:50:0, 20:80:0, 0:80:20, 0:50:50 and 0:20:80 mixture solution, errors and corrections) for all numbers of neurons (4, 5, 6, 7, 8 and 9) in hidden layer of the feed-forward backpropagation neural network is shown in Table 1. The minimum mean error of NaCl in KCl, NaCl and

$BaCl_2$ mixture solution can be shown at 7 neurons in hidden layer of the feed-forward backpropagation neural network, this error is about 2.4676 % and the correction (1-error) is about 97.5323 %. Therefore, the 7 neurons in hidden layer of the feed-forward backpropagation neural network is used in the program to get more accurate results. These programs can be setup on a computer and connected to experimental setup of liquid flow system with SH-SAW sensor to get automatically results of mixing ratio of KCl, NaCl and $BaCl_2$ of mixture solution which has the same conductivity (σ = 0.5 S/m).

CONCLUSIONS

In this paper, determination of mixing ratios of KCl, NaCl and $BaCl_2$ of solution which has the same conductivity (σ = 0.5 S/m) using Shear Horizontal Surface Acoustic Wave (SH-SAW) and Neural Network are presented. Experimental results of liquid flow system with SH-SAW sensor are taken. A computer programs based on the feed-forward backpropagation neural network is built.

The minimum mean error of NaCl in KCl, NaCl and $BaCl_2$ solution can be shown at 7 neurons in hidden layer of the feed-forward backpropagation neural network. This error is about 2.4676 % and the correction (1-error) is about 97.5323 %. Therefore, the 7 neurons in hidden layer of the feed-forward backpropagation neural network is used in the program to get more accurate results. These programs can be set up on a computer and connected to experimental set up of liquid flow system with SH-SAW sensor to get automatically results of mixing ratio of KCl, NaCl and $BaCl_2$ solution which has the same conductivity (σ = 0.5 S/m).

REFERENCES

1. M. Rapp, B. Bob, A. Voigt, H. Gemmeke, H. J. Ache, Fresenius J. Anal. Chem., **352**, 1995, 699-704.
2. M. Penza, P. Aversa, G. Cassano, W. Wlodarski, K. Kalantar-Zadeh, Sensors and Actuators B, **127**, 2007, 168–178.
3. S. J. Martin, A. J. Ricco, T. M. Niemczyk, G. C. Frye, Sensors and Actuators, **20**, 1989, 253-268.
4. M. Saad Zaghloul, Taha Elsayed Taha, Aly H. A. Moustafa, Khamies El-Shennawy, IEEE Transactions on Instrumentation and Measurement, **50**, 2001, 95-100.
5. J. Kondoh, T. Muramatsu, T. Nakanishi, Y. Matsui, S. Shiokawa, Sensors and Actuators B, **92**, 2003, 191–198.
6. S. J. Martin, A. J. Ricco, Sensors and Actuators A, **21**, 1990, 712-718.
7. W.D. Hunt, C. Corso, NNIN REU Research Accomplishments, 2005.
8. Youngjune Hur, Jinho Han, Jooheon Seon, Yukeun Eugene Pak, Yongrae Roh, Sensors and Actuators A, **120**, 2005, 462–467.
9. A. Tsortos, E. Gizeli, Biosensors and Bioelectronics, **24**, 2008, 836–841.
10. E. Howe, G. Harding, Biosensors & Bioelectronics, **15**, 2000, 641–649.
11. Ku-Shang Chang, Chen-Kai Chang, Chien-Yuan Chen, Sensors and Actuators B, **125**, 2007, 207–213.
12. M. Bisoffi, B. Hjelle, D.C. Brown, Biosensors and Bioelectronics, **23**, 2008, 1397–1403.
13. N. Moll, E. Pascal, D.H. Dinh, ITBM-RBM, **29**, 2008, 155–161.
14. T.M.A. Gronewold, U. Schlecht, E. Quandt, Biosensors and Bioelectronics, **22**, 2007, 2360–2365.
15. Kai Ge, Dezhong Liu, Shouzhuo Yao, Fresenius J Anal Chem, **354**, 1996, 118–121.
16. Qingyun Cai, Ronghui Wang, Shouzhuo Yao, Mikrochim. Acta., **126**, 1997, 109–115.
17. Taha E. Taha, Mohamed A. A. El-Dosoky, Ahmed M. El-Sayed, The 24th National Radio Science Conference (NRSC), Cairo, Egypt, 2007, 1-8.
18. Michael Thompson, David C.Stone, Surface-Launched Acoustic Wave Sensors, John Wiley & Sons Inc., 1997.
19. S.Datta, Surface Acoustic Wave Devices, Prentice-Hall,Englewood Cliffs. NJ., 1986.
20. Woon-Seng Gan, Sen M. Kuo, Embedded Signal Processing with the Micro Signal Architecture, John Wiley & Sons Inc, 2007.
21. Ch.S. Lessard, Signal Processing of Random Physiological Signals, Morgan & Claypool Publishers series, 2006.
22. A.B. Watson, NASA Ames Research Center, Mathematica Journal, **4**, 1994, 81-88.
23. T. Yamazaki, J. Kondoh, Y. Matsui, S. Shiokawa, Sensors and Actuators A, **83**, 2000, 34–39.
24. J. Kondoh, Y. Matsui, S. Shiokawa, Sensors and Actuators B, **91**, 2003, 309-315.
25. M.M. Gupta, L. Jin, N. Homma, Static and Dynamic Neural Networks From Fundamentals to Advanced Theory, John Wiley & Sons Inc., 2003.